

Review Article

Theme: Translational Application of Nano Delivery Systems: Emerging Cancer Therapy
Guest Editors: Mahavir B. Chougule and Chalet Tan

Light-Activatable Gold Nanoshells for Drug Delivery Applications

Burapol Singhana,^{1,2} Patrick Slattery,³ Aaron Chen,⁴ Michael Wallace,¹ and Marites P. Melancon^{1,5,6}

Received 22 October 2013; accepted 28 January 2014; published online 19 February 2014

Abstract. Gold nanoshells (AuNSs) are currently being investigated as nanocarriers for drug delivery systems and have both diagnostic and therapeutic applications, including photothermal ablation, hyperthermia, drug delivery, and diagnostic imaging, particularly in oncology. AuNSs are valuable for their localized surface plasmon resonance, biocompatibility, low immunogenicity, and facile functionalization. AuNSs used for drug delivery can be spatially and temporally triggered to release controlled quantities of drugs inside the target cells when illuminated with a near-infrared (NIR) laser. Recently, many research groups have demonstrated that these AuNS complexes are able to deliver antitumor drugs (*e.g.*, doxorubicin, paclitaxel, small interfering RNA, and single-stranded DNA) into cancer cells, which enhances the efficacy of treatment. AuNSs can also be functionalized with active targeting ligands such as antibodies, aptamers, and peptides to increase the particles' specific binding to the desired targets. This article reviews the current research on NIR light-activatable AuNSs used as nanocarriers for drug delivery systems and cancer theranostics.

KEY WORDS: drug delivery; gold nanoshells; nanocarrier; theranostics; triggered release.

INTRODUCTION

Gold nanoshells (AuNSs) have emerged as innovative platforms in nanomedicine and have been intensively investigated for cancer therapeutics and diagnostics (theranostics) and drug delivery systems. AuNSs are nanoparticles composed of an organic (polymer or lipid) or inorganic (metal) core coated with a thin layer of gold. AuNSs can also be hollow. These thin AuNSs possess optical localized surface plasmon resonance, an electromagnetic mode associated with the collective oscillation of free electrons in conduction bands (1,2). The optical properties of AuNSs such as absorption and scattering depend on the size and shape of the nanoparticles (2,3). Therefore, the plasmon of AuNSs can be tuned from the visible region of the spectrum to the physiological "water window" in the near-infrared (NIR) region (650–900 nm) of the spectrum by changing the core size as well as the thickness

and composition of the gold shells (3). The resonance optical properties of AuNSs in NIR light are an attractive characteristic for biomedical applications because water and naturally occurring fluorochromes have the lowest absorption coefficients in this region. Therefore, these properties allow light to penetrate deeper into the tissues (3,4). Furthermore, AuNSs have a high-absorption cross-section for stably and efficaciously converting absorbed light into heat, which can be used in the photothermal ablation (PTA) of cancers (5). In addition, owing to their scattering properties, AuNSs can be utilized in diagnostic imaging as contrast-enhanced reagents for computed tomography, optical coherence tomography, dark-field microscopy, and photoacoustic tomography (2,6,7).

AuNSs' physicochemical properties have been also investigated, as AuNSs have potential as an alternative nanocarrier for drug delivery systems. Researchers have reported that, by releasing their payload only after being triggered by NIR irradiation, AuNSs mediate the controlled release of chemotherapeutic agents or biological drugs (*e.g.*, DNA/RNA) into the desired targets, thereby increasing a drug's efficacy while decreasing its unwanted side effects (8–12).

In addition, their versatile gold–thiol chemistry allows the particles' gold shells to be easily functionalized with a wide variety of targeting ligands, including small organic or inorganic molecules (*e.g.*, folates, sugars, and carbohydrates), antibodies, aptamers, and peptides, which makes actively targeted AuNSs potentially suitable platforms for therapeutic nanomedicine (13–15).

Several advantages are gained from using nanoparticles as delivery vehicles rather than conventional drug delivery systems. First, they can protect drugs from biodegradation in

¹ Department of Interventional Radiology, The University of Texas MD Anderson Cancer Center, 1515 Holcombe Boulevard, Houston, Texas 77030, USA.

² The Faculty of Liberal Arts and Sciences, Nakhon Phanom University, Nakhon Phanom, Thailand.

³ College of Medicine, Northeast Ohio Medical University, Rootstown, Ohio, USA.

⁴ The University of Texas Medical School at Houston, Houston, Texas, USA.

⁵ The University of Texas Graduate School of Biomedical Sciences at Houston, Houston, Texas, USA.

⁶ To whom correspondence should be addressed. (e-mail: mmelancon@mdanderson.org)

the body and prolong the *in vivo* half-lives of drugs, resulting in enhanced efficacy. Second, nanoparticles can improve the solubility of hydrophobic drugs. Third, nanoparticles can reduce potential immunogenicity. Lastly, they can be engineered to release drugs at target sites with predetermined and/or tunable release rates or in response to external stimuli triggers (12,16). In particular, solid gold nanoparticles (AuNPs) have been studied as drug delivery systems owing to their biocompatibility, low toxicity, and unique localized surface plasmon resonance (1,12,17). The payloads of these AuNPs could be small-molecule drugs or large biomolecules such as DNA (8), RNA (9), or doxorubicin (DOX) (18). Recently, hollow AuNSs (HAuNSs) have emerged as a new effective nanocarrier for drug delivery (19,20).

This review focuses on current research on the ability of AuNSs, both silica-cored (Si@AuNSs) and HAuNSs, to be highly effective nanocarriers for drug delivery systems, particularly in cancer theranostics. We discuss the ability of both types of AuNSs for passive and active targeting to improve anticancer drug delivery and treatment efficacy by delivering cytotoxic/biological drugs to malignant cells and releasing the drugs when triggered with NIR laser irradiation. The PTA and other theranostic applications of Si@AuNSs, HAuNSs, and other nanomaterials are not the focus of this chapter; excellent reviews about these particles can be found elsewhere (3,6,21–25).

Gold-Based Nanoshells

The first-generation Si@AuNSs were first described by Halas' group (26,27). The Si@AuNSs from their studies consisted of a dielectric silica core surrounded by a thin noble metal shell. Because of their inherent localized surface plasmon resonance properties, Si@AuNSs have been studied for diagnostic imaging and photothermal cancer therapy (5,28) and have advanced into clinical trials under the brand name AuroLase (3,6). Furthermore, Halas' group has investigated the use of Si@AuNSs as drug carriers for cancer treatment (29).

Since the introduction of Si@AuNSs, a myriad of AuNS structures, including HAuNSs, magnetic-coated AuNSs (Fe₃O₄@AuNSs and FePt@AuNSs), polymer-cored AuNSs (poly(lactic-co-glycolic acid) [PLGA]@AuNSs), and phospholipid/liposome-cored AuNSs have been synthesized (Table I). The morphologies, sizes, and chemical compositions of these AuNSs have been controlled precisely. Some of them have been extensively studied for their physicochemical properties, and a few have been used in biomedical applications. For instance, You *et al.* reported that HAuNSs show promise for PTA therapy and for achieving the controlled release of DOX inside cancer cells (18).

GOLD NANOSHELLS FOR DRUG DELIVERY

Smart, multifunctional nanocarriers for directed release of controlled quantities of active molecules inside the target cells are in high demand for drug delivery systems. AuNSs possess the properties necessary to be used as a single platform for theranostic applications owing to their optical plasmon resonance. Spatially and temporally controlled release of drugs/biological agents from AuNSs into the cellular tissues

can be accomplished using NIR irradiation. Several studies have focused on the use of AuNSs for NIR-activated release of drugs in biomedical applications, particularly cancer treatments. In this section, we elaborate on the use of AuNSs for both passively and actively targeted drug delivery systems.

Passively Targeted AuNSs for Chemotherapeutic Drug Delivery






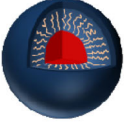
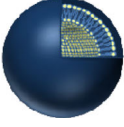
In general, AuNSs and other AuNPs that are intravenously administered passively accumulate in tumors because of their enhanced permeability and retention (EPR), the hallmarks of which are leaky vasculature and minimal lymphatic drainage (14). The exploitation of this mechanism requires particles that have long half-lives that prolong the anticancer agent's circulation time to increase its efficacy (38). Therefore, AuNSs are normally functionalized with polyethylene glycol (PEG) to enhance their biodistribution and evade the mononuclear phagocyte system (MPS). Chemical or biological payloads can be embedded inside or immobilized on AuNSs, depending on the morphology of the AuNSs. For example, payloads can be both encapsulated inside and immobilized on the surface of HAuNSs.

Recently, HAuNSs have gained attention as a new single platform for drug delivery systems owing to their synergistic capabilities as photothermal agents for PTA and as drug carriers for drug delivery. Furthermore, their NIR plasmon resonance wavelength can be used as a remote trigger for manipulating the drug delivery system. Their small size (30–50 nm in diameter), absence of a silica core, spherical shape, strong and tunable (520–950 nm) absorption band, and lack of a need for surfactant for stabilization provide HAuNSs with great potential for cancer theranostic applications (18–20,39).

You *et al.* hypothesized that the unique photothermal conversion property of HAuNSs could be harnessed for modulating the delivery of anticancer drugs, thus making it possible to achieve significantly enhanced antitumor efficacy using a combination of PTA and chemotherapy (photochemotherapy) in a single platform (18,39,40). Li's group proposed that HAuNSs could be used as a nanocarrier to ferry DOX, a commercially available chemotherapeutic agent, to the tumor cells. In the study of Li's group (18), HAuNSs were synthesized by sacrificial galvanic replacement of cobalt nanoparticles in the presence of chloroauric acid, as described in a previous report (30,40). Approximately 40 nm HAuNSs was made and coated with PEG. After that, both PEG-coated HAuNSs and HAuNSs were mixed with DOX for 24 h at room temperature and then washed repeatedly to produce DOX@PEG-HAuNSs and DOX@HAuNSs. Their morphology and ultraviolet–visible absorption were evaluated using a transmission electron microscope and ultraviolet–visible spectrometer, as shown in Fig. 1. The researchers found that PEGylation of HAuNSs enhanced their physical stability without affecting their plasma resonance peaks (Fig. 1b). The researchers also reported that the percentage of encapsulated DOX could be as high as 63% by weight (~1.7 μg DOX/μg Au) *via* the electrostatic interaction between inner/outer gold shell surfaces and DOX molecules, as compared with percentage by weight for DOX on AuNSs (18).

NIR light-induced release of DOX@HAuNSs was also investigated in this study (18). After irradiation with an

Table I. Summary of Gold-Based Nanoshells

Nanoparticle	Structure	Core	References
Silica-core AuNS (Si@AuNS)		Silica (SiO ₂)	26,27
Hollow AuNS (HAuNSs)		-	30,31
Magnetic-coated, silica-core AuNS (Fe ₃ O ₄ @SiO ₂ @AuNS)		Iron oxide (Fe ₃ O ₄) coated with SiO ₂	32
Magnetic-core AuNS (FePt@AuNS)		Iron platinum (FePt)	33
Polymer-core AuNS (PLGA@AuNS)		Poly (lactic-co-glycolic acid) (PLGA)	34,35
Quantum dot-core AuNS (QD@AuNS)		Quantum dot (QD) coated with lipid	36
Liposome-core AuNS (LAuNS)		Liposome (phospholipid)	37

808-nm NIR laser, the quantity of DOX released was monitored, as shown in Fig. 2a. The intensity peak at 490 nm, which is the absorption peak of DOX, was increased when DOX@HAuNSs was irradiated with a laser. Furthermore, no DOX release from DOX-coated AuNSs was observed, as shown in Fig. 2b, because AuNSs do not possess plasma absorption in the NIR region. In addition, no DOX release from DOX@HAuNSs was observed without irradiating these particles with the NIR laser (Fig. 2c). These results indicated

that the presence of NIR light might be responsible for NIR laser-triggered release of DOX from DOX@HAuNSs. In addition, they also pointed out that HAuNSs have a higher capacity for DOX binding than nanospheres of the same size because DOX molecules can diffuse into the core and bind to the inner surface of HAuNSs (Fig. 2d).

In an *in vitro* cell uptake study, both DOX@HAuNS and DOX@PEG-HAuNS were internalized into human MDA-MB-231 breast cancer cells and were retained in the

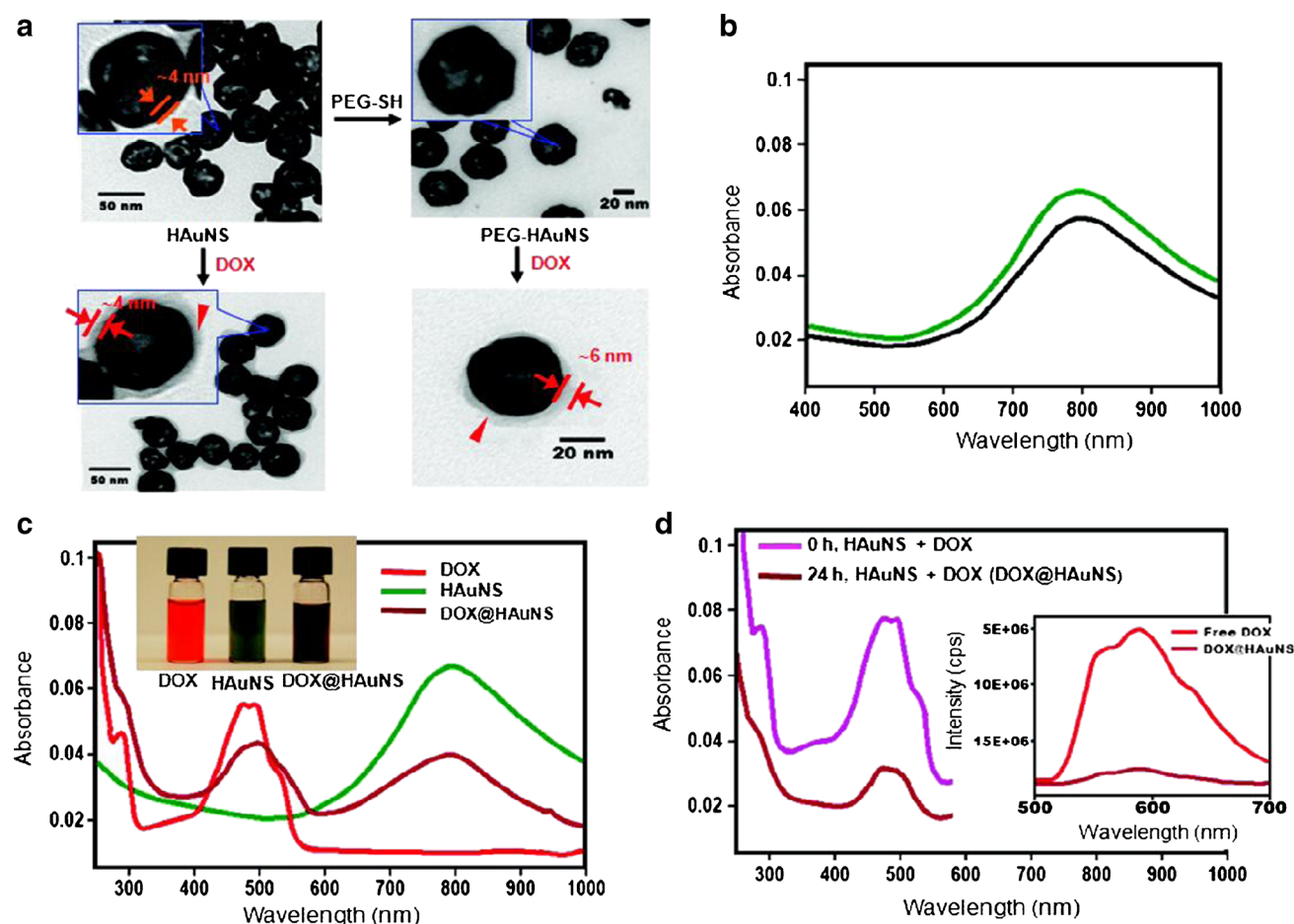


Fig. 1. Physico-chemical characteristics of DOX-loaded HAuNSs. **a** Transmission electron microscope images depicted DOX covering the surface of both DOX@HAuNS and DOX@PEG-HAuNS, which did not exist in HAuNS and PEG-HAuNS before DOX coating. **b** Ultraviolet-visible absorption spectra exhibited that the plasmon resonance peak of PEG-HAuNSs (*black line*) did not change as compared with bare AuNSs (*green line*). **c** The color of the HAuNS changed from greenish to henna upon absorption of DOX. DOX@HAuNS displayed an ultraviolet-visible absorption peak at 490 nm, which is characteristic of DOX, and a broad NIR plasmon absorption peak at ~ 800 nm, which is characteristic of HAuNS. **d** At 24 h after mixing, the absorbance peak intensity of DOX in the ultraviolet-visible region was significantly reduced compared with the absorbance peak intensity immediately after mixing DOX and HAuNS (0 h) owing to the quenching effect. In addition, compared with free DOX, which exhibited strong fluorescence emission, the fluorescence signal from DOX in DOX@HAuNS was almost completely quenched (**d, inset**). These results indicate that DOX was tightly bound to HAuNS and PEG-HAuNS after 24 h of incubation. Reproduced with permission from ref. (18). Copyright 2010, American Chemical Society (ACS)

endolysosomal compartments (18). NIR laser irradiation (1.0 W/cm^2 for 3 min per treatment, four treatments over a 2-h period) caused the release of DOX from DOX@HAuNS, and DOX was distributed to cell nuclei (Fig. 3). Thus, it is possible to control intracellular DOX release from DOX@HAuNS and DOX@PEG-HAuNS by using NIR laser irradiation. In addition, researchers found that, after NIR irradiation, the number of DOX@HAuNS and DOX@PEG-HAuNS in the cells increased significantly. These DOX nanoshell complexes exhibited a significantly enhanced cell killing effect toward cancer cells owing to both photothermal heat and the cytotoxic activity of DOX.

The pharmacokinetics and biodistribution of DOX@PEG-HAuNSs *in vitro* and *in vivo* using MDA-MB-231 and A2780 ovarian cancer cells were also reported by You *et al.* (19). *In vitro*, DOX@PEG-HAuNSs released DOX immediately and mediated PTA upon NIR laser treatment. In addition, *in vivo*, DOX@PEG-HAuNSs accumulated in tumor cells at a higher

rate than free DOX and showed greater antitumor activity than free DOX or liposomal DOX when irradiated with an NIR laser (Fig. 4). Again, this single nanoplatform combining PTA and a chemotherapeutic drug shows promise for enhanced cancer efficacy owing to the synergistic cytotoxic effect of DOX released from PEG-HAuNSs and the photothermal effect mediated by HAuNSs.

Furthermore, Lee *et al.* (41) demonstrated an approach to monitoring *in vitro* and *in vivo* real-time DOX release from DOX@PEG-HAuNSs upon irradiation with an NIR laser using fluorescent optical imaging and photoacoustic imaging techniques for tracking DOX and HAuNSs, respectively (41). *In vitro*, the release of DOX was initiated with a 3-W laser. *In vivo*, DOX@PEG-HAuNSs were injected intratumorally or intravenously into 4T1 tumor-bearing nude mice. After 24 h, fluorescence optical imaging (emission wavelength = 600 nm, excitation wavelength = 500 nm) and photoacoustic imaging were used to track the internalized particles. They found that

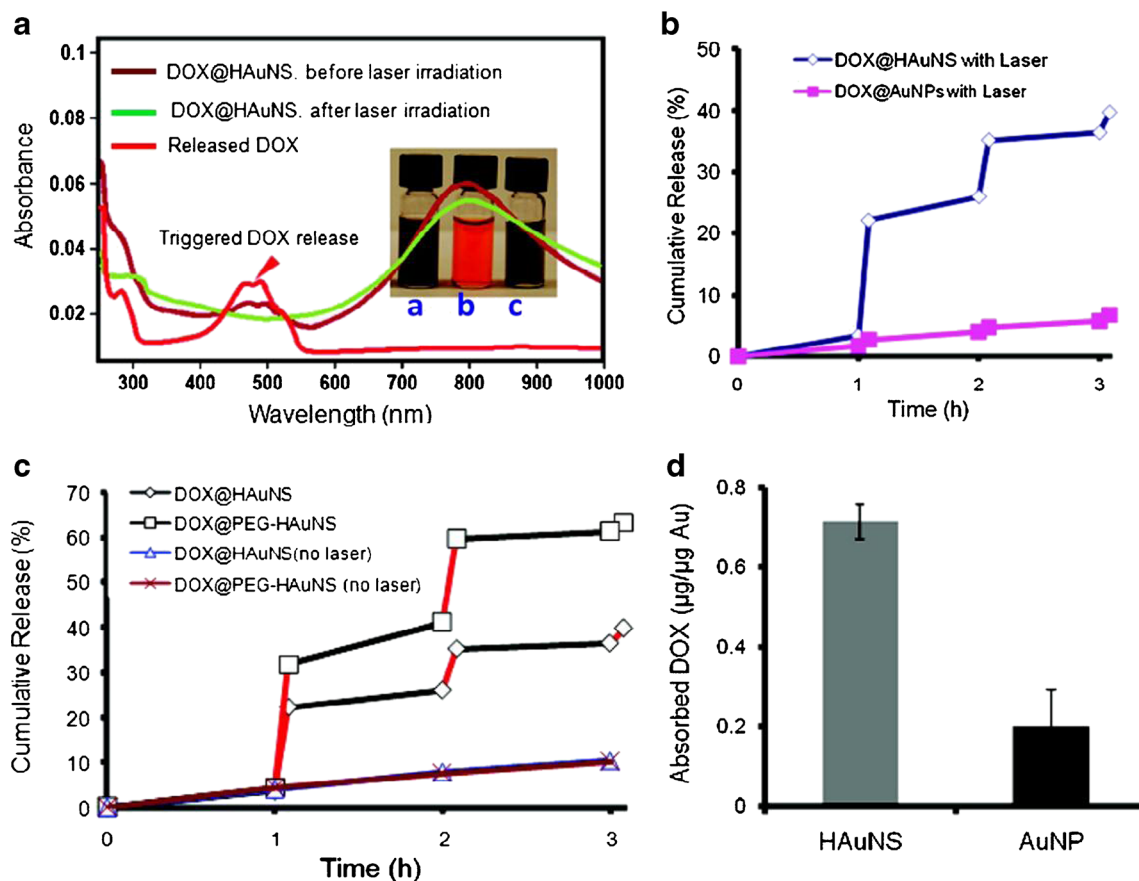


Fig. 2. Release profile of DOX from HAuNS complexes when irradiated with an 808-nm NIR laser. **a** Ultraviolet-visible spectra of DOX@HAuNS before and after NIR laser irradiation. *Inset* photograph of aqueous solutions of *a* DOX@HAuNS before laser irradiation, *b* released DOX collected in the supernatant, and *c* DOX@HAuNS after complete release of DOX. **b** Release of DOX from DOX@HAuNS (*blue line*) and DOX@AuNP (*pink line*) under repeated NIR laser exposure. **c** NIR light-triggered release of DOX from DOX@HAuNS and DOX@PEG-HAuNS with and without NIR laser irradiation. Rapid DOX release was observed during NIR exposure (5 min, *red lines*), and the release was turned off when the laser was switched off. **d** DOX payload was higher in HAuNS than in solid AuNS. Reproduced with permission from ref. (18). Copyright 2010, ACS

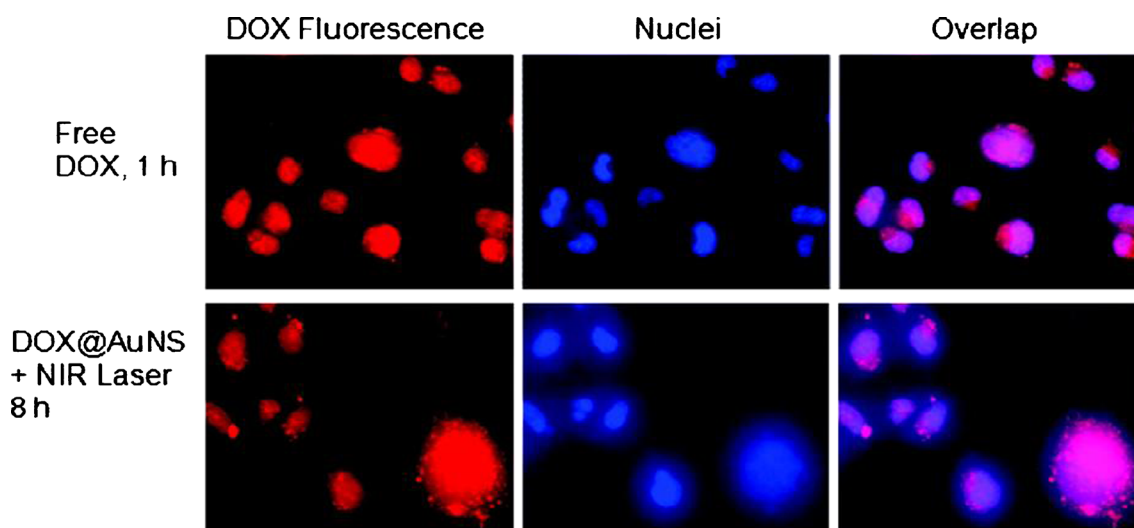


Fig. 3. *In vitro* imaging of DOX@HAuNS and free DOX in MDA-MB-231 breast cancer cells. Cell uptake of free DOX and DOX@HAuNS treated with an 808-nm NIR laser ($1.0 \text{ W}/\text{cm}^2$ for 3 min per treatment, four treatments over 2 h, incubated for 8 h). Cell nuclei were counterstained with 4',6-diamidino-2-phenylindole (DAPI; *blue*). The red fluorescence signal from DOX in DOX@HAuNS was localized to the cell nuclei after NIR laser irradiation, indicating intracellular release of DOX from DOX@HAuNS upon NIR exposure. Reproduced with permission from ref. (18). Copyright 2010, ACS

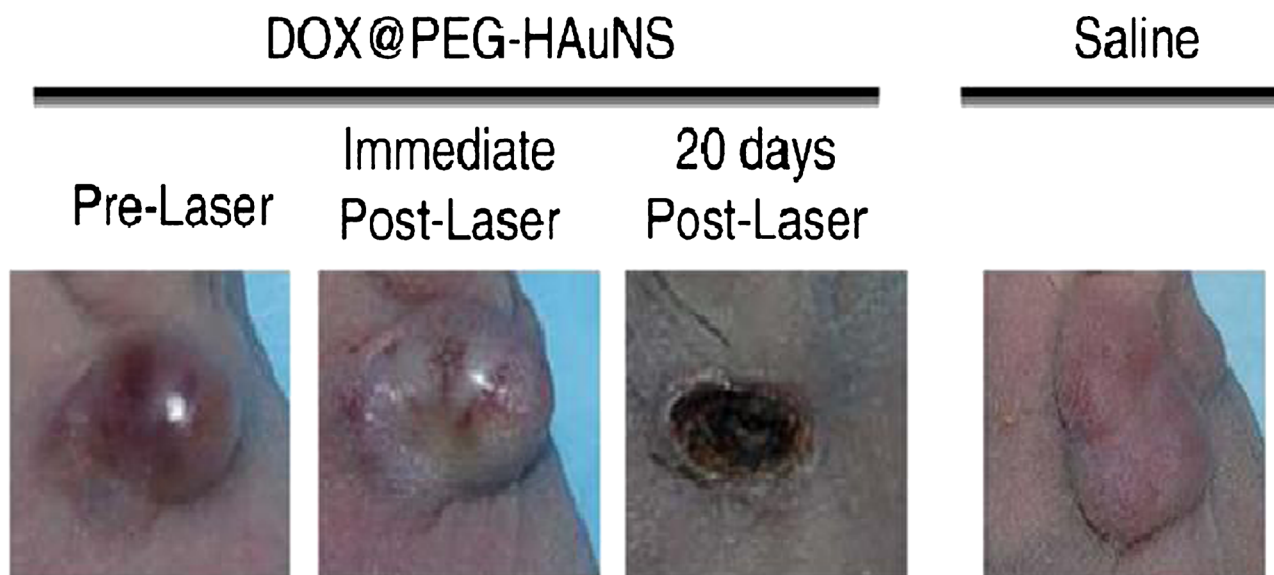


Fig. 4. Antitumor activity *in vivo* of DOX@PEG-HAuNSs plus laser treatment against an MDA-MB-231 tumor. The tumor growth was slowed by treatment with the HAuNS complex and laser irradiation. Reproduced with permission from ref. (19). Copyright 2012, Elsevier

the fluorescence intensity in surface laser-treated tumors 24 h after treatment was significantly higher than that in untreated tumors ($p=0.015$ for intratumoral, $p=0.008$ for intravenous), as shown in Fig. 5a. Photoacoustic imaging (acquisition

wavelength=800 nm) revealed that laser treatment caused a substantial increase in tumor temperature, from 37°C to ablative temperatures of >50°C (Fig. 5b, c). In addition, *ex vivo* analysis revealed that the fluorescence intensity of laser-

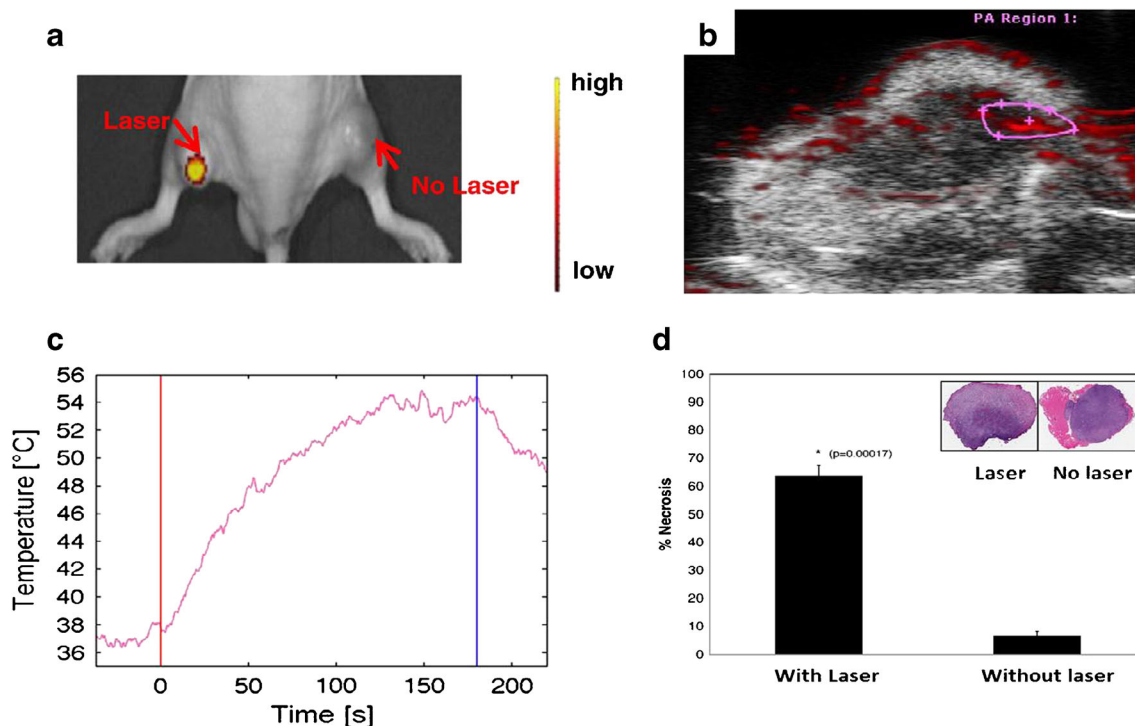


Fig. 5. *In vivo* fluorescence intensity studies. **a** Representative *in vivo* fluorescence optical imaging of DOX release following the intratumoral injection of DOX@PEG-HAuNS at $t=24$ h. **b** Overlaid photoacoustic and B-mode images of DOX release *in vivo* following intratumoral injection of DOX@PEG-HAuNS (1.32×10^{12} particles/mL) and treatment with a 6-W surface laser. **c** Conversion of photoacoustic signal to temperature. The first vertical line indicates the start of laser treatment, and the second vertical line indicates the end of laser treatment. **d** Histological analysis. The percentage of tumor necrosis in laser-treated mice (64%) was significantly higher than that in untreated mice (7%). Inset representative hematoxylin and eosin-stained slides of 4T1 tumors injected intratumorally with DOX@PEG-HAuNS with and without NIR surface laser treatment (0.15 W/mm^2 for 1 min). Reproduced with permission from ref. (41). Copyright 2013, Elsevier

treated tumors was twice as high as that of untreated tumors ($p=0.009$), as shown in Fig. 5d. On the basis of these findings, Lee *et al.* concluded that fluorescence optical imaging and photoacoustic imaging show promise as approaches for assessing DOX release and monitoring temperature, respectively, after DOX@PEG-HAuNS-mediated thermal ablation therapy.

In addition, HAuNSs have been used for the triggered release of antitumor paclitaxel encapsulated in PLGA microspheres (20). Researchers found that the release of paclitaxel from the polymeric microspheres was readily controlled by the output power of the NIR laser.

Liposomal AuNSs for temporally and spatially controlled drug delivery have been fabricated using DOX-loaded liposomes as a core coated with gold shells (37). Researchers found that, upon NIR irradiation, the liposomal AuNSs collapsed and DOX was released from the liposomes. They also found that this liposomal AuNS nanocarrier provided leakage-free, overextended storage and is monodisperse and compact in size.

Actively Targeted AuNSs for Chemotherapeutic Drug Delivery

Despite DOX@PEG-HAuNSs' promise of enhanced cancer efficacy *via* the EPR effect of tumors, their short circulation

half-lives and nonspecific binding to tumor cells make them a less-than-ideal treatment. More importantly, not all tumors exhibit the EPR effect (38,42), which severely limits the effective use of AuNSs in such tumors. For example, the central regions of metastatic tumors do not have the EPR effect owing to poor vasculature, which leads to a low accumulation of colloidal AuNSs. Thus, AuNSs alone have insufficient therapeutic efficacy.

However, AuNSs' anticancer efficacy can be improved using a targeted delivery strategy. This approach can also reduce the toxic side effects of treatment to healthy cells. AuNSs can be attached to targeting moieties, which can bind specifically and selectively to receptors that are overexpressed on the tumor cell surface to facilitate the tumor cell's internalization of AuNSs (*i.e.*, receptor-mediated endocytosis). In addition, to increase the treatment efficacy of AuNSs, researchers can use thiol-gold coupling chemistry to modify the surface of the particles' gold shells (43). A wide range of actively targeting ligands, including antibodies, aptamers, peptides, sugars, and carbohydrates, and small molecules (*i.e.*, folic acid or folates) can be attached to the gold shell surfaces (13,15,38,44,54). These ligands target the markers specific for a particular cancer type, such as receptors overexpressed on their surfaces, to improve the anticancer efficacy of AuNSs. In

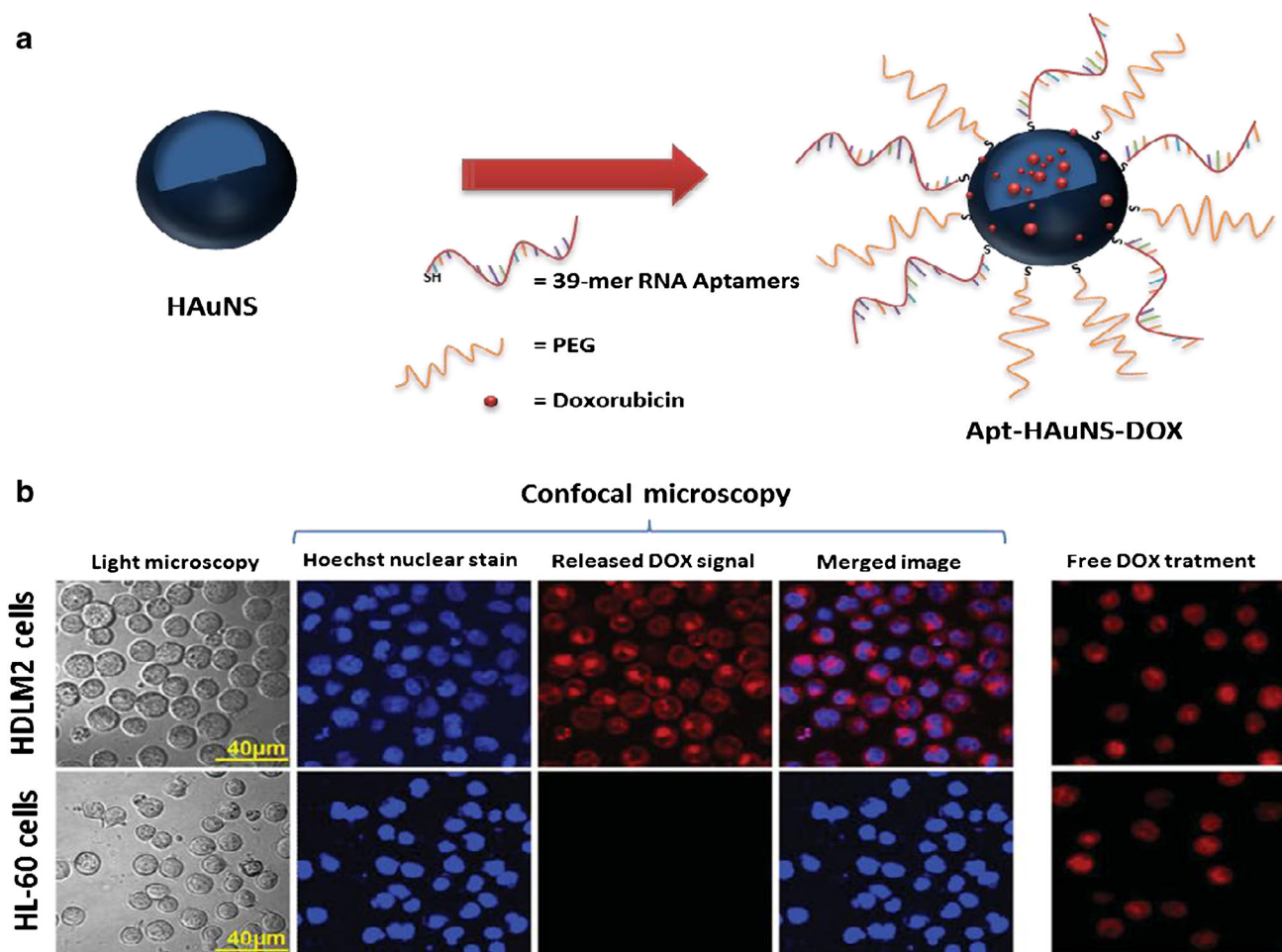


Fig. 6. **a** Apt-HAuNS-DOX synthesis. **b** *Top row* Apt-HAuNS-DOX bound specifically to HDLM2 lymphoma cells and released the DOX (*red*) intracellularly. Hoechst 33342 was used for nuclear staining (*blue*). *Bottom row* Apt-HAuNS-DOX did not bind to HL-60 cells, which do not express CD30 biomarkers. Free DOX treatment was the control. Adapted from ref. (10), and used with permission. Copyright 2013, Wiley

cancer treatment, the main goals in using targeted AuNSs are to maximize the accumulation of AuNSs in malignant cells and to minimize their accumulation in nonmalignant cells.

To take advantage of a targeted delivery strategy, researchers have also conjugated 39-mer RNA specific for CD30 (a CD30-expressing anaplastic large cell lymphoma cell line) to DOX-loaded HAuNSs (Apt-HAuNS-DOX). These targeted HAuNSs bound specifically to HDLM2 lymphoma cells and released the loaded DOX intracellularly but did not bind to HL-60 cells, which lack the expression of CD30 biomarkers (Fig. 6). The release of DOX by Apt-HAuNS-DOX was stimulated by the acidic pH condition of lysosomes. Importantly, the Apt-HAuNS-DOX selectively killed lymphoma cells without affecting nontargeted cells in the same cultures (10).

Besides the 39-mer RNA aptamer described previously, antibodies are another popular targeting ligand, which have been conjugated to the gold shell surfaces to enhance anticancer efficacy (54). For instance, researchers have fabricated drug-loaded polymeric AuNSs (DPGNSs) that have been used as templates for polymer-coated AuNSs (34). These DPGNSs include a targeting multifunctional PLGA-conjugated AuNS loaded with DOX and cetuximab (CET-DPGNS) (34). Cetuximab is a chimeric monoclonal antibody that tar-

gets the epidermal growth factor receptor (EGFR), which is a cell surface receptor that is overexpressed in most cancers (45). The researchers found that, *in vitro*, both CET-DPGNSs and CET-PGNSs exhibited higher toxicity to A431 cells than did immunoglobulin G PGNSs or immunoglobulin G DPGNSs because the cetuximab-targeting ligand bound specifically to EGFR, which is overexpressed on the surface of A431 tumor cells. In addition, owing to the remote-controlled burst release of cytotoxic DOX from the DPGNSs, CET-DPGNSs were more cytotoxic to A431 cells than were CET-PGNSs (which did not encapsulate DOX) after incubation for 24 h and NIR laser irradiation. This enhanced necrosis is attributed to the synergistic effect of PTA and the cytotoxicity of DOX.

The cyclic TNYLFSPNGPIARAW peptide (c(TNYL-RAW)), a second-generation ephrin type-B receptor 4 (EphB4)-binding antagonist that has improved plasma stability and high receptor-binding affinity as compared with its acyclic peptide parent, was conjugated to multifunctional DOX@HAuNSs that target EphB4 (Fig. 7a). The c(TNYL-RAW)-DOX@HAuNS increased accumulation in three EphB4-positive tumors both *in vitro* and *in vivo*. Compared with treatments with nontargeted DOX@HAuNS or HAuNS

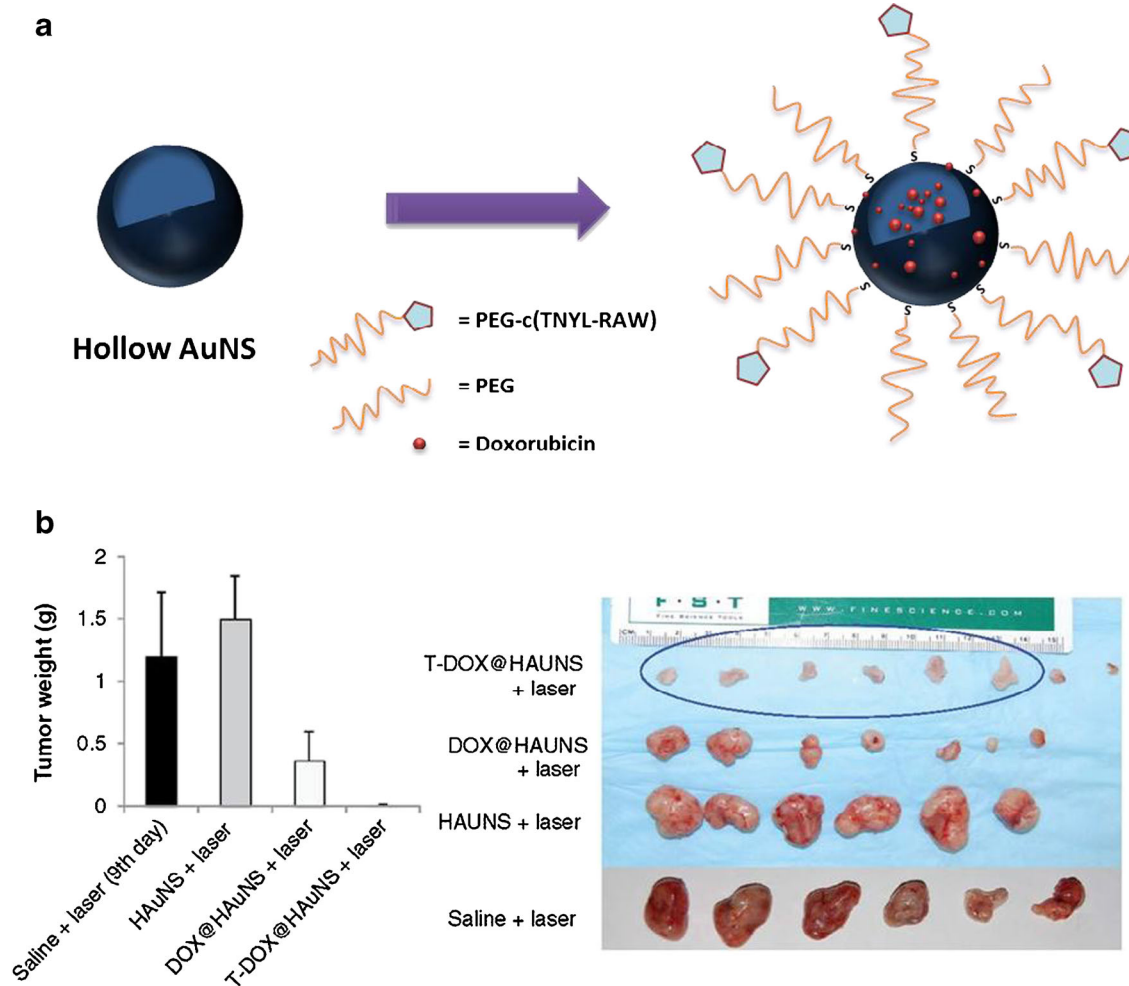


Fig. 7. **a** SH-PEG-c(TNYL-RAW)-conjugated, DOX-loaded HAuNSs for targeted photothermal chemotherapy. **b** The average weights of tumors from different treatment groups. Reproduced with permission from ref. (46). Copyright 2012, American Association for Cancer Research (AACR)

followed by NIR laser irradiation, treatment with c(TNYL-RAW)-DOX@HAuNSs followed by NIR laser irradiation resulted in significantly slower tumor growth (Fig. 7b) (46).

GOLD NANOSHELLS FOR GENE DELIVERY

Passively Targeted AuNSs for Gene Delivery

Using AuNSs for gene delivery has enormous advantages over other treatment techniques (8,47) that use ultraviolet-visible light to remotely trigger the release of a gene. Without AuNSs, these techniques are difficult to apply to *in vivo* gene silencing because tissues absorb ultraviolet-visible light. NIR irradiation can be used to induce the release of siRNA/DNA

from AuNSs at the illuminated site, reducing the nonspecific effects and providing tools for kinetic studies, off-target effect assessment, and phenotypic assay. In addition, the attachment of siRNA/DNA also protects AuNSs from nucleases, resulting in good cellular uptake (8).

Halas' group extensively investigated Si@AuNSs for spatially and temporally controlled delivery of drugs into targeted cell lines. They proposed that double-stranded DNA (dsDNA) attached to Si@AuNSs was dehybridized and released the nonthiolated antisense sequence upon NIR irradiation at the AuNS plasmon resonance wavelength. These dsDNA nanoshell complexes (dsDNA-AuNSs) also showed promise in drug delivery systems as an effective host and for the light-triggered release of drug molecules (8,17,47). Guest

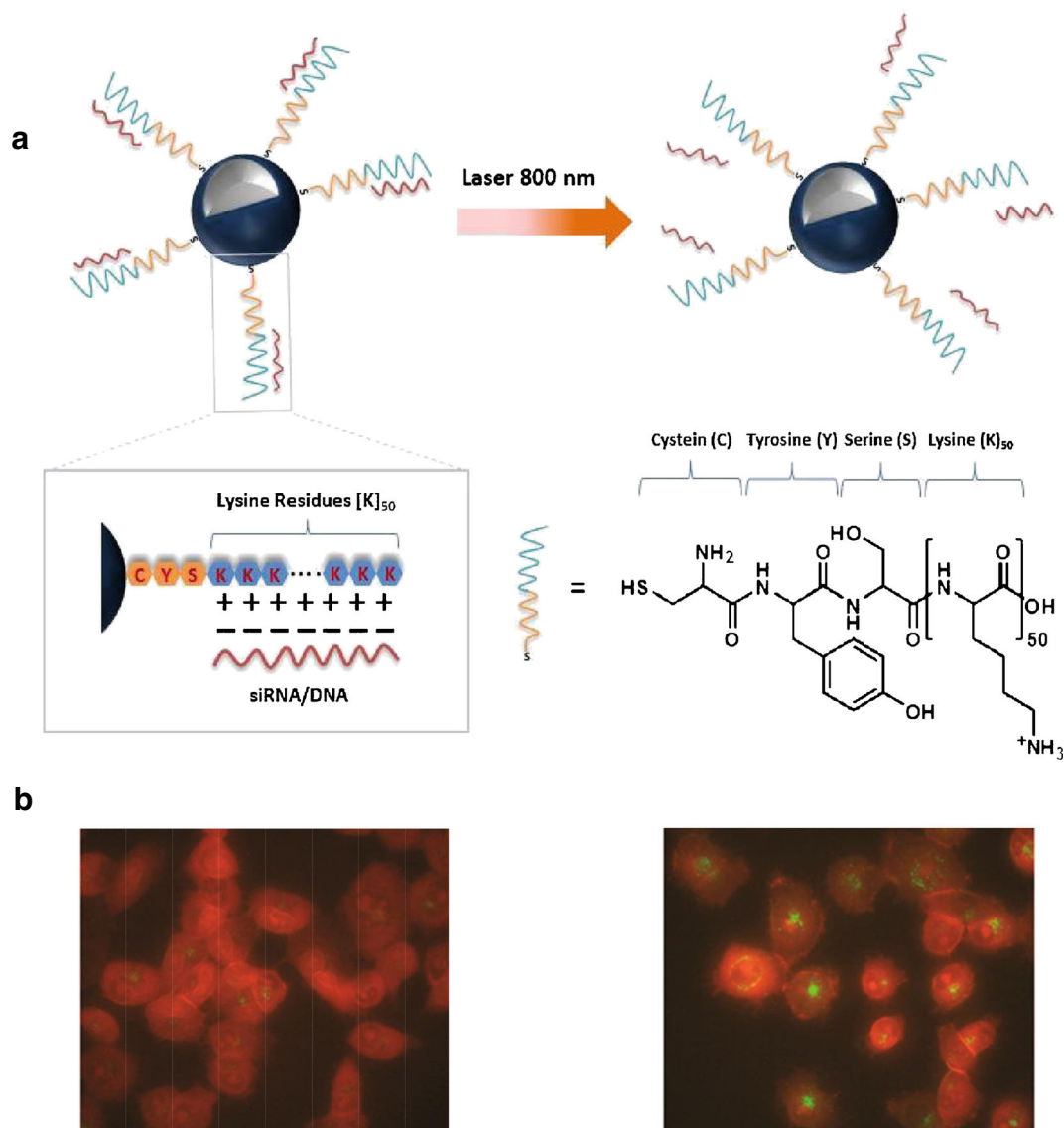


Fig. 8. a Si@AuNS poly-L-lysine-based therapeutic RNA interference oligonucleotide delivery system. The negatively charged phosphate backbone of the siRNA/ssDNA (red) is electrostatically attached to the cationic peptide (blue), which consists of one cysteine, one tyrosine, one serine, and 50 lysine amino acids. Upon NIR irradiation, the siRNA/ssDNA is released. b Fluorescence images of H1299 cells incubated with ssDNA-Si@AuNSs. Alexa Fluor 488 (green) was used to fluorescently label the ssDNA. Without illumination with an NIR laser (without laser treatment), Alexa Fluor 488 was quenched by the AuNS surface, indicating that there is no dehybridization/release of ssDNA. The release of ssDNA after illumination with an NIR laser (with laser treatment). Adapted and reproduced with permission from ref. (49). Copyright 2012, ACS

molecules can associate with dsDNA either by intercalating between adjacent base pairs or by binding in either the major or minor groove of the DNA double helix. Host–guest association can be assembly driven by using hydrogen bonding, π – π bond interactions, van der Waals forces, dipole–dipole interactions, and electrostatic interactions (48). Cargo release was increased when dsDNA–AuNS complexes were triggered with NIR irradiation (17).

Moreover, the use of dsDNA–AuNSs in the on-demand, light-triggered, remote-controlled delivery of DNA or RNA oligonucleotides in gene therapy has been widely investigated (3,11,17,49). For instance, Halas' group (49) investigated the use of Si@AuNSs coated with poly-L-lysine as therapeutic oligonucleotide delivery vehicles (Fig. 8a). The researchers coated Si@AuNSs with poly-L-lysine to provide Si@AuNSs with the positive charge necessary for forming an electrostatic interaction with the negatively charged antisense single-stranded DNA (ssDNA) and siRNA oligonucleotides. Upon application of an 800-nm NIR laser, this Si@AuNS complex delivered the antisense ssDNA and siRNA oligonucleotides intracellularly to H1299 cells, as shown in Fig. 8b (49).

Actively Targeted AuNSs for Gene Delivery

Lu *et al.* (11) designed multifunctional HAuNSs that deliver DNA or RNA *via* a light-induced release system (Fig. 9). Folic acid targeting a folate receptor on the cancer cells was integrated into the multifunctional HAuNSs carrying siRNA. This siRNA specifically recognizes a nuclear factor- κ B (NF- κ B) transcription factor that is related to the expression of genes involved in tumor development (50). HAuNSs (40 nm) were conjugated with thiol-modified siRNA duplexes directed toward the NF- κ B p65 subunit. Foliates were coupled to the nanoparticles through a thioctic acid-terminated PEG linker to generate F-PEG-HAuNS-siRNA (Fig. 9a). Intravenous injection of these HAuNSs into HeLa xenografts followed by irradiation with an 800-nm pulsed NIR laser resulted in the distinct downregulation of the NF- κ B p65 subunit only for the folate-conjugated HAuNS treatment owing to selective targeting (Fig. 9b). In addition, researchers demonstrated that the pulsed NIR laser-dependent release of siRNA from Tat lipid-coated AuNSs resulted in the spatiotemporal silencing of a reporter gene (green fluorescence protein) *in vitro* (9).

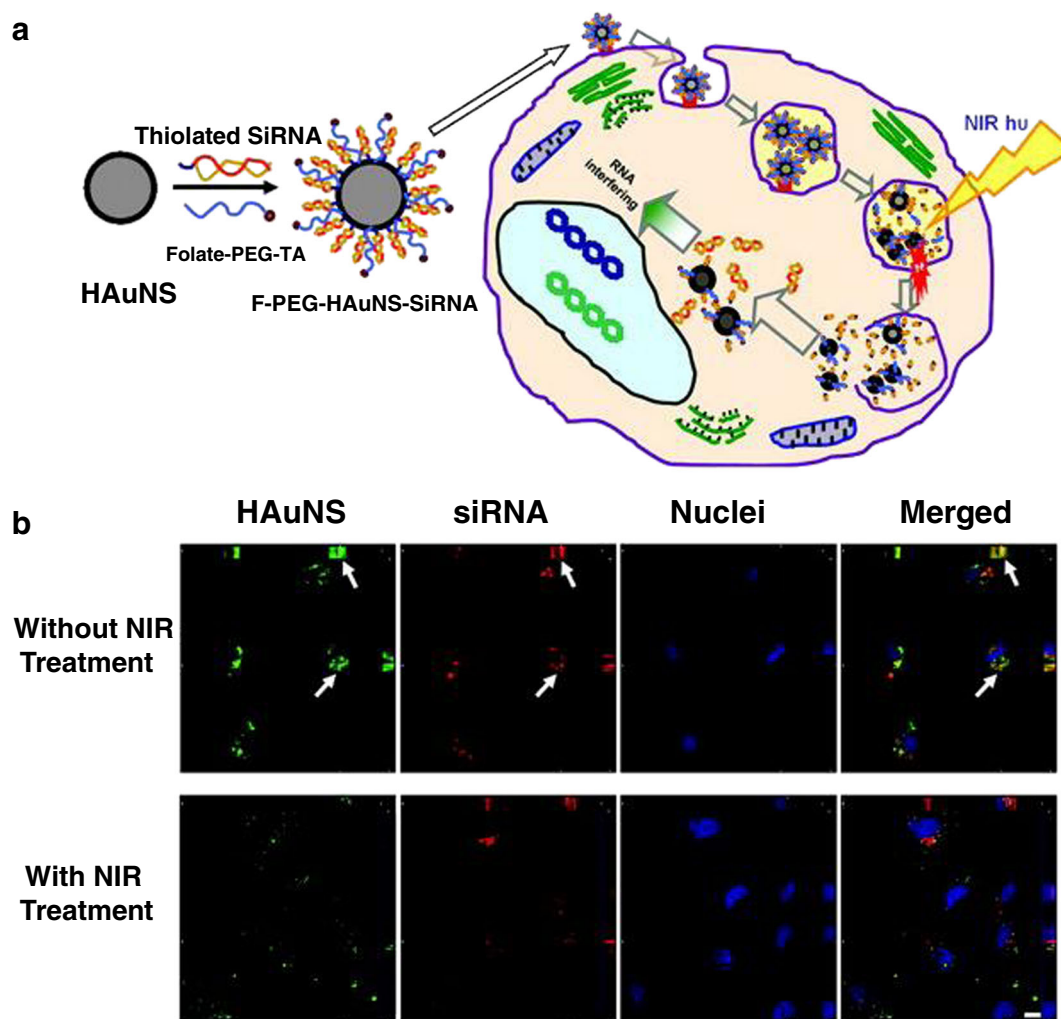


Fig. 9. **a** The synthetic scheme of F-PEG-HAuNS-siRNA and their proposed intracellular itinerary following NIR light irradiation. **b** *In vitro* fluorescence imaging showed the dissociation of siRNA from HAuNS after laser irradiation. Red Dy547-labeled siRNA, green scattering signal of HAuNS, blue cell nuclei counterstained with DAPI. Arrows siRNA colocalized with HAuNS. Reproduced with permission from ref. (11). Copyright 2010, AACR

OUTLOOK

AuNSs show promise as highly effective nanoplatforms for drug delivery systems and theranostic applications in this nanotechnology era. Owing to their inherent localized surface plasmon resonance, AuNSs can be utilized to absorb light for PTA therapy. They can also carry therapeutic payloads and imaging agents for the simultaneous diagnosis and treatment of a disease. In addition, they can release these agents when irradiated with NIR light. AuNSs' NIR plasmon resonance allows an NIR laser to be used as a remote control to spatially and temporally trigger the release of drugs from the AuNSs into the target area. Several studies have shown cancer treatment efficacy with both the *in vitro* and *in vivo* use of AuNSs plus NIR laser treatment. Integrating a targeting moiety such as an antibody, aptamer, or peptide onto the surface of AuNSs also enhances the particles' theranostic efficacy by increasing their accumulation in targeted tumor cells.

In conclusion, photochemotherapy using AuNSs, by combining PTA therapy and chemotherapy in a single platform, is a promising strategy for drug delivery, particularly in the treatment of cancer. AuNS complexes demonstrate enhanced anticancer efficacy and diminished toxicity. In addition, these nanocomplexes can be manipulated for spatially and temporally triggered release of treatment agents by using NIR irradiation. Given the advancement in conjugation techniques, a wide range of targeting ligands can now be conjugated to AuNSs, resulting in highly effective theranostic platforms for delivering active compounds into the diseased cells. In the near future, targeted AuNSs could have a significant impact not only on cancer therapy but also on the treatment of cardiovascular (51,52) and immunological diseases (53). For instance, vascular cell adhesion molecule 1 (VCAM-1)-conjugated AuNS was used as a probe for photoacoustic imaging of atherosclerotic plaques in mice (51). Researchers found that targeting VCAM-1 AuNSs selectively accumulated in atherosclerotic-prone regions in mice, which represents an adequate means to target atherosclerotic plaques in small animals. These results lead to a new method to observe the effect of therapies on the progression or regression of the disease.

ACKNOWLEDGMENTS

The authors thank Luanne Jorewicz in MD Anderson's Department of Scientific Publications for editing the manuscript. This work was supported in part by a grant from the John S. Dunn Foundation and by the National Institutes of Health through MD Anderson's Cancer Center Support Grant CA016672.

REFERENCES

1. Link S, El-Sayed MA. Optical properties and ultrafast dynamics of metallic nanocrystals. *Annu Rev Phys Chem.* 2003;54:331–6.
2. Halas NJ, Lal S, Link L, Chang W-S, Natelson D, Hafner JH, *et al.* A plethora of plasmonics from the laboratory for nanophotonics at Rice University. *Adv Mater.* 2012;24:4842–77.
3. Bardhan R, Lal S, Joshi A, Halas NJ. Theranostic nanoshells: from probe design to imaging and treatment of cancer. *Acc Chem Res.* 2011;44:936–46.
4. Weissleder R. A clearer vision for *in vivo* imaging. *Nat Biotechnol.* 2001;19:316–7.
5. Hirsch LR, Stafford RJ, Bankson JA, Sershen SR, Rivera B, Price RE, *et al.* Nanoshell-mediated near-infrared thermal therapy of tumors under magnetic resonance guidance. *P Natl Acad Sci.* 2003;100:13549–54.
6. Lal S, Clare SE, Halas NJ. Nanoshell-enabled photothermal cancer therapy: impending clinical impact. *Acc Chem Res.* 2008;41:1842–51.
7. Melancon MP, Zhou M, Li C. Cancer theranostics with near-infrared light-activatable multimodal nanoparticles. *Acc Chem Res.* 2011;44:947–56.
8. Barhoumi A, Huschka R, Bardhan R, Knight MW, Halas NJ. Light-induced release of DNA from plasmon-resonant nanoparticles: towards light-controlled gene therapy. *Chem Phys Lett.* 2009;482:171–9.
9. Braun GB, Pallaoro A, Wu G, Missirlis D, Zasadzinski JA, Tirrell M, *et al.* Laser-activated gene silencing *via* gold nanoshell-siRNA conjugates. *ACS Nano.* 2009;3:2007–15.
10. Zhao N, You J, Zeng Z, Li C, Zu Y. An ultra pH-sensitive and aptamer-equipped nanoscale drug-delivery system for selective killing of tumor cells. *Small.* 2013;9:3477–84.
11. Lu W, Zhang G, Zhang R, Flores II LG, Huang Q, Gelovani JG, *et al.* Tumor site-specific silencing of NF- κ B p65 by targeted hollow gold nanosphere-mediated photothermal transfection. *Cancer Res.* 2010;70:3177–88.
12. Zhang Z, Wang J, Chen C. Near-infrared light-mediated nanoplatforms for cancer thermo-chemotherapy and optical imaging. *Adv Mater.* 2013;25:3869–80.
13. Alexander-Bryant AA, Vanden Berg-Foels WS, Wen X. Bioengineering strategies for designing targeted cancer therapies. *Adv Cancer Res.* 2013;118:1–59.
14. Kievit FM, Zhang M. Cancer nanotheranostics: improving imaging and therapy by targeted delivery across biological barriers. *Adv Mater.* 2011;23:H217–47.
15. Cheng Z, Zaki AA, Hui JZ, Muzykantov VR, Tsourkas A. Multifunctional nanoparticles: cost versus benefit of adding targeting and imaging capabilities. *Science.* 2012;338:903–10.
16. Shi J, Votruba AR, Farokhzad OC, Langer R. Nanotechnology in drug delivery and tissue engineering: from discovery to applications. *Nano Lett.* 2010;10:3223–30.
17. Huschka R, Neumann O, Barhoumi A, Halas NJ. Visualizing light-triggered release of molecules inside living cells. *Nano Lett.* 2010;10:4117–22.
18. You J, Zhang G, Li C. Exceptionally high payload of doxorubicin in hollow gold nanospheres for near-infrared light-triggered drug release. *ACS Nano.* 2010;4:1033–41.
19. You J, Zhang R, Zhang G, Zhong M, Liu Y, Van Pelt CS, *et al.* Photothermal chemotherapy with doxorubicin-loaded hollow gold nanospheres: a platform for near-infrared light-triggered drug release. *J Control Release.* 2012;158:319–28.
20. You J, Shao R, Wei X, Gupta S, Li C. Near-infrared light triggers release of paclitaxel from biodegradable microspheres: photothermal effect and enhanced antitumor activity. *Small.* 2010;6:1022–31.
21. Jin Y. Multifunctional compact hybrid Au nanoshells: a new generation of nanoplasmonic probes for biosensing, imaging, and controlled release. *Acc Chem Res.* 2013. doi:10.1021/ar400086e.
22. Xia X, Wang Y, Ruditskiy A, Xia Y. 25th Anniversary article: galvanic replacement: a simple and versatile route to hollow nanostructures with tunable and well-controlled properties. *Adv Mater.* 2013;25:6313–33.
23. Boisselier E, Astruc D. Gold nanoparticles in nanomedicine: preparations, imaging, diagnostics, therapies, and toxicity. *Chem Soc Rev.* 2009;38:1759–82.
24. Eustis S, El-Sayed MA. Why gold nanoparticles are more precious than pretty gold: noble metal surface plasmon resonance and its enhancement of the radiative and nonradiative properties of nanocrystals of different shapes. *Chem Soc Rev.* 2006;35:209–17.
25. Dreaden EC, Mackey MA, Huang X, Kangy B, El-Sayed MA. Beating cancer in multiple ways using nanogold. *Chem Soc Rev.* 2011;40:3391–404.
26. Averitt RD, Sarkar D, Halas NJ. Plasmon resonance shifts of Au-coated Au₂S nanoshells: insight into multicomponent nanoparticle growth. *Phys Rev Lett.* 1997;78:4217–20.

27. Oldenberg SJ, Averitt RD, Westcott SL, Halas NJ. Nanoengineering of optical resonances. *Chem Phys Lett.* 1998;288:243–7.
28. Loo C, Lin A, Hirsch L, Lee M-H, Barton J, Halas NJ, *et al.* Nanoshell-enabled photonics-based imaging and therapy of cancer. *Technol Cancer Res Treat.* 2004;3:33–40.
29. Chen W, Bardhan R, Bartels M, Perez-Torres C, Pautler RG, Halas NJ, *et al.* A Molecularly targeted theranostic probe for ovarian cancer. *Mol Cancer Ther.* 2010;9:1028–38.
30. Liang HP, Wan LJ, Bai CL, Jiang L. Gold hollow nanospheres: tunable surface plasmon resonance controlled by interior-cavity sizes. *J Phys Chem B.* 2005;109:7795–800.
31. Prevo BG, Esakoff SA, Mikhailovsky A, Zasadzinski JA. Scalable routes to gold nanoshells with tunable sizes and response to near-infrared pulsed-laser irradiation. *Small.* 2008;4:1183–95.
32. Ji XJ, Shao RP, Elliott AM, Stafford RJ, Esparza-Coss E, Bankson JA, *et al.* Bifunctional gold nanoshells with a superparamagnetic iron oxide-silica core suitable for both MR imaging and photothermal therapy. *J Phys Chem C.* 2007;111:6245–51.
33. Nandwana V, Elkins KE, Poudyal N, Chaubey GS, Yano K, Liu JP. Size and shape control of monodisperse FePt nanoparticles. *J Phys Chem C.* 2007;111:4185–9.
34. Yang J, Lee J, Kang J, Oh SJ, Ko H-J, Son J-H, *et al.* Smart drug-loaded polymer gold nanoshells for systemic and localized therapy of human epithelial cancer. *Adv Mater.* 2009;21:4339–42.
35. Dong W, Li Y, Niu D, Ma Z, Gu J, Chen Y, *et al.* Facile synthesis of monodisperse superparamagnetic Fe₃O₄ core@hybrid@Au shell nanocomposite for bimodal imaging and photothermal therapy. *Adv Mater.* 2011;23:5392–7.
36. Jin YD, Gao XH. Plasmonic fluorescent quantum dots. *Nat Nanotechnol.* 2009;4:571–6.
37. Jin Y, Gao X. Spectrally tunable leakage-free gold nanocontainers. *J Am Chem Soc.* 2009;131:17774–6.
38. Kamaly N, Xiao Z, Valencia PM, Radovic-Moreno AF, Farokhzad OC. Targeted polymeric therapeutic nanoparticles: design, development and clinical translation. *Chem Soc Rev.* 2012;47:2971–3010.
39. Melancon MP, Stafford RJ, Li C. Challenges to effective cancer nanotheranostics. *J Control Release.* 2012;164:177–82.
40. Lu W, Xiong C, Zhang G, Huang Q, Zhang R, Cheng JZ, *et al.* Targeted photothermal ablation of murine melanomas with melanocyte-stimulating hormone analog-conjugated hollow gold nanospheres. *Clin Cancer Res.* 2009;15:876–86.
41. Lee HJ, Liu Y, Zhao J, Zhou M, Bouchard RR, Mitcham T, *et al.* *In vitro* and *in vivo* mapping of drug release after laser ablation thermal therapy with doxorubicin-loaded hollow gold nanoshells using fluorescence and photoacoustic imaging. *J Control Release.* 2013;172:152–8.
42. Nagamitsu A, Greish K, Maeda H. Elevating blood pressure as a strategy to increase tumor-targeted delivery of macromolecular drug SMNCS: cases of advanced solid tumors. *Jpn J Clin Oncol.* 2009;39:756–66.
43. Love JC, Kriebel JK, Nuzzo RG, Whitesides GM. Self-assembled monolayers of thiolates on metals as a form of nanotechnology. *Chem Rev.* 2005;105:1103–69.
44. Peer D, Karp JM, Hong S, Farokhzad OC, Margalit R, Langer R. Nanocarriers as an emerging platform for cancer therapy. *Nat Nanotechnol.* 2007;2:751–60.
45. Herbst RS. Review of epidermal growth factor receptor biology. *Int J Radiat Oncol Biol Phys.* 2004;59:S21–6.
46. You J, Zhang R, Xiong C, Zhong M, Melancon MP, Gupta S, *et al.* Effective photothermal chemotherapy using doxorubicin loaded gold nanospheres that target EphB4 receptors in tumors. *Cancer Res.* 2012;72:4777–86.
47. Huschka R, Zuloaga J, Knight MW, Brown LV, Nordlander P, Halas NJ. Light-induced release of DNA from gold nanoparticles: nanoshells and nanorods. *J Am Chem Soc.* 2011;133:12247–55.
48. Neto BAD, Lapis AAM. Recent developments in the chemistry of deoxyribonucleic acid (DNA) intercalators: principles, design, synthesis, applications and trends. *Molecules.* 2009;14:1725–46.
49. Huschka R, Barhoumi A, Liu Q, Roth JA, Ji L, Halas NJ. Gene silencing by gold nanoshell-mediated delivery and laser-triggered release of antisense oligonucleotide and siRNA. *ACS Nano.* 2012;6:7681–91.
50. Karin M, Cao Y, Greten FR, Li ZW. NF- κ B in cancer: from innocent bystander to major culprit. *Nat Rev Cancer.* 2002;2:301–10.
51. Rouleau L, Bertia R, Ng VWK, Matteau-Pelletiera C, Lamd T, *et al.* VCAM-1-targeting gold nanoshell probe for photoacoustic imaging of atherosclerotic plaque in mice. *Contrast Media Mol Imaging.* 2013;8:27–39.
52. Spivak MY, Bubnov RV, Yemets IM, Lazarenko LM, *et al.* Gold nanoparticles—the theranostic challenge for PPPM: nanocardiology application. *EPMA J.* 2013;4:1–17.
53. Smith DM, Simon JK, Baker Jr JR. Applications of nanotechnology for immunology. *Nat Rev Immunol.* 2013;13:592–605.
54. Melancon MP, Lu W, Yang Z, Zhang R, *et al.* *In vitro* and *in vivo* targeting of hollow gold nanoshells directed at epidermal growth factor receptor for photothermal ablation therapy. *Mol Cancer Ther.* 2008;7:1730–9.